ADVANCING EARTH AND SPACE SCIENCES

JGR Earth Surface

RESEARCH ARTICLE
10.1029/2024JF008126

Land-To-Sea Sediment Fluxes From a Major Glacial Lake Outburst Flood Were Stepped Rather Than Instantaneous

L. P. Bailey[1,2], **D. H. Shugar**[1,3], **M. Tilston**[1,3], **S. M. Hubbard**[1], **I. Giesbrecht**[3], **J. Del Bel Belluz**[3], **J. M. Jackson**[3,4], **M. A. Clare**[5], **M. J. B. Cartigny**[6], **S. Açıkalın**[7], **S. Hage**[8], **P. J. Talling**[6], **H. Basiuk**[1], **B. Menounos**[3,9], **and M. Geertsema**[10]

[1]Department of Earth, Energy, and Environment, University of Calgary, Calgary, AB, Canada, [2]School of Ocean and Earth Science, University of Southampton, Southampton, UK, [3]Hakai Institute, Quadra Island, BC, Canada, [4]Fisheries and Oceans Canada, Sidney, BC, Canada, [5]Ocean BioGeosciences, National Oceanography Centre, Southampton, UK, [6]Department of Geography and Earth Sciences, Durham University, Durham, UK, [7]School of Natural and Environmental Sciences, Newcastle University, Newcastle, UK, [8]GEOPS, UMR 8148, Université Paris-Saclay, Saclay, France, [9]Department of Geography, Earth, and Environmental Sciences, University of Northern British Columbia, Prince George, BC, Canada, [10]British Columbia Institute of Technology, Prince George, BC, Canada

Key Points:

- A glacial lake outburst flood occurred on 28 November 2020 delivering ~4.3×10^6 m^3 of sediment into the marine environment of Bute Inlet
- Days after the outburst flood minor increases in sea surface turbidity were observed with much larger increases lagging 5 months later
- Sediment was stored and remobilised during elevated river discharge, delaying the onshore-to-offshore transport of sediment

Correspondence to:
L. P. Bailey,
Lewis.Bailey@uCalgary.ca

Citation:
Bailey, L. P., Shugar, D. H., Tilston, M., Hubbard, S. M., Giesbrecht, I., Del Bel Belluz, J., et al. (2025). Land-to-sea sediment fluxes from a major glacial lake outburst flood were stepped rather than instantaneous. *Journal of Geophysical Research: Earth Surface*, *130*, e2024JF008126. https://doi.org/10.1029/2024JF008126

Received 6 NOV 2024
Accepted 25 MAR 2025

Author Contributions:
Conceptualization: L. P. Bailey, D. H. Shugar, S. M. Hubbard
Data curation: J. Del Bel Belluz
Formal analysis: L. P. Bailey, D. H. Shugar, M. Tilston
Funding acquisition: L. P. Bailey, D. H. Shugar, M. A. Clare
Investigation: L. P. Bailey, D. H. Shugar, M. Tilston, S. M. Hubbard, I. Giesbrecht, J. Del Bel Belluz, J. M. Jackson
Methodology: L. P. Bailey
Resources: I. Giesbrecht, J. Del Bel Belluz
Supervision: D. H. Shugar, M. Tilston, S. M. Hubbard
Visualization: L. P. Bailey, H. Basiuk
Writing – original draft: L. P. Bailey, D. H. Shugar
Writing – review & editing: M. Tilston, S. M. Hubbard, I. Giesbrecht, J. Del Bel Belluz, J. M. Jackson, M. A. Clare,

Abstract

Glacial lake outburst floods can transport large volumes of sediment. Where these floods reach the coastline, much of the particulate matter is delivered directly to the marine environment. It has been suggested that offshore deposits, specifically in fjord settings, may provide a faithful record of past outburst flood events. However, a lack of observations means that the mechanics and the timing of sediment transport offshore following a glacial lake outburst event remain poorly constrained. Here, we document the changes in sea surface sediment dynamics following the 28 November 2020 Elliot Lake outburst flood in British Columbia, which transported ~4.3×10^6 m^3 of sediment into an adjacent fjord (Bute Inlet) as a deep nepheloid layer directly following the event. However, analysis of sea surface turbidity using in situ measurements and satellite-derived estimates reveals that changes in fjord-head surface turbidity in the months following the major flood were surprisingly small. The highest measured sea surface turbidity instead occurred 5 months after the initial outburst flood. This delayed increase in seaward sediment flux coincided with the onset of the spring freshet, when the discharge of the rivers feeding Bute Inlet increases each year. We suggest that large quantities of sediment were temporarily stored within the river catchment and were only remobilized when river discharge exceeded a threshold level following seasonal snowmelt. Our results reveal a temporal disconnect, where onshore to offshore transfer of sediment is stepped following a glacial lake outburst flood, which could complicate the sedimentology of subsequent deposits.

Plain Language Summary

Human-driven climate change is melting glaciers; in turn, this is increasing the size and number of glacial lakes, both of which are set to continue increasing in the future. Sometimes these lakes drain suddenly in what is known as a glacial lake outburst flood. These floods are highly erosive and can transport material many hundreds of km downstream, and even into the ocean if they occur near the coast. Here, we document the impact of an outburst flood that occurred near the coast of British Columbia, Canada on 28 November 2020, which eroded and transported a very large quantity of sediment into the ocean. By analysing satellite images and measuring sediment concentrations in surface seawater, we show that suspended sediment near the coast shows surprisingly little change immediately after the flood in contrast to large initial subsurface transport. Instead, we observed a delayed peak in seawater surface sediment 5 months after the initial outburst flood. This peak was higher than in previous years due to sediment stored in the river catchment following the outburst flood. The stepped delivery of sediment to the ocean raises questions about the offshore deposits of glacial lake outburst floods.

1. Introduction

The acceleration of global glacier retreat in response to climate change (Hugonnet et al., 2021) is changing sediment transport processes (Zhang et al., 2022). Glacial retreat is driving a rapid increase in the size and number of glacial lakes (Ahmed et al., 2021; Shugar et al., 2020; Wilson et al., 2018) and the subsequent debuttressing of valley walls is increasing the likelihood of landslides (Deline et al., 2021). Consequently, it has been suggested that the frequency of glacial lake outburst floods could increase over the coming decades, though whether such increases will occur remains somewhat contested (Carrick & Tweed, 2016; Harrison et al., 2018;

M. J. B. Cartigny, S. Açıkalın, S. Hage, P. J. Talling, H. Basiuk, B. Menounos, M. Geertsema

Vandekerkhove et al., 2020; Veh et al., 2020; Wilson et al., 2018). Glacial lake outburst floods can generate potentially catastrophic floods, following the sudden release of glacial lake meltwater. These floods therefore have considerable transport potential, whereby large quantities of sediment are eroded and redistributed, resulting in large-scale geomorphic changes downstream (Carrivick & Tweed, 2016; Clague & Evans, 2000; Cook et al., 2018; Sattar et al., 2025; Tomczyk et al., 2020; Tweed & Russell, 1999; Veh et al., 2020), and potentially beyond, into the submarine realm when glacial lakes are proximal to the coast (Piret et al., 2022; Vandekerkhove et al., 2021). Such outburst floods therefore pose a significant threat to human populations and infrastructure for tourism, commerce, communications, energy and food security in glacierized mountain ranges (Carrivick & Tweed, 2016; Clague & Evans, 2000; Meerhoff et al., 2019; Sattar et al., 2025; Taylor et al., 2023).

Fjords are highly susceptible to changes following glacial lake outburst floods. For example, changes in fjord water stratification and suspended sediment concentrations have been observed following outburst events, whereby the entire fjord ecosystem can be impacted (Geertsema et al., 2022; Marín et al., 2013; Meerhoff et al., 2019). Such abrupt changes, coupled with the potential of fjord sediments to record high-resolution changes in climate (Bianchi et al., 2020; Howe et al., 2010), have led to the suggestion that fjords could provide an archive of past outburst floods (Vandekerkhove et al., 2021). However, there is an assumption that a direct and instantaneous connection exists between outburst flood discharge and offshore sediment transport (e.g., Prior et al., 1987), yet the temporal resolution (e.g., from radiometric dating techniques) has inhibited testing of this hypothesis.

Here, we analyse sea surface observations to investigate changes in offshore sediment dynamics following a large glacial lake outburst flood near Bute Inlet, British Columbia (Figures 1a and 1d). An outburst flood occurred ~10 km upstream of the inlet on 28 November 2020 when $\sim 11 \times 10^6$ m^3 of rock entered proglacial "Elliot Lake" (informal name) at the head of Elliot Creek (a tributary of the Southgate River; Figure 1a) following a rockslide along the steep valley wall (Donati et al., 2022; Geertsema et al., 2022). The impact of the rockslide produced a >100 m run-up wave, causing water to overtop the lake outlet, scouring a 10-km-long channel (Figure 1b), and producing a 2 km^2 ($\sim 4 \times 10^6$ m^3 volume) depositional fan below (Figures 1a and 1c). The event delivered an additional $\sim 4.3 \times 10^6$ m^3 of sediment into the marine environment at Bute Inlet (Figure 1a), creating an extensive surface sediment plume below a water depth of 200 m (Geertsema et al., 2022). Similar surface sediment plumes close to the river mouth feeding the fjord have previously been shown to generate turbidity currents (sediment gravity flows; Hage et al., 2019; Hizzett et al., 2018). These turbidity currents dominate the onshore-to-offshore flux of sediment and organic material in Bute Inlet (and other sub-polar to temperate fjords) in the absence of catastrophic events, and are more important than submerged delta-front landslides for triggering turbidity currents (Bailey et al., 2023; Bornhold et al., 1994; Clare et al., 2016; Hage et al., 2022; Heijnen et al., 2020, 2022; Hizzett et al., 2018; Normandeau et al., 2019; Piret et al., 2024; Pope et al., 2022). Such surface sediment plume-triggered turbidity currents have also been attributed to relatively small-scale glacial lake outburst floods (e.g., Vandekerkhove et al., 2021), volcanic lake outburst floods offshore from small Pacific islands (e.g., Clare et al., 2018), and even the formation of some of the largest sedimentary fan deposits downstream of former ice sheets (Bellwald et al., 2020). However, a lack of observations both before and after a major glacial lake outburst flood exist (e.g., Jacquet et al., 2017), meaning our knowledge of how and when sediment transfers from land to sea is poorly constrained.

In this study, we address this knowledge gap by quantifying sea surface turbidity (i.e., the "cloudiness" of water caused by suspended sediment content) both prior to, and following, the 2020 Elliot Lake outburst flood. Surface water turbidity was collected directly using in situ surface water measurements from 2018 to 2022 ($n = 42$) and estimated using 38-year of optical satellite images ($n = 320$; Figure 2). First, we identify patterns and controls on nearshore sea surface turbidity in Bute Inlet prior to this outburst flood. This provides an insight to the background variability and the seasonal controls on sediment transport. Second, we analyse spatial and temporal changes in turbidity in the 2 years following the outburst flood to document instantaneous and delayed effects on offshore sediment fluxes. Finally, we present a new model to explain the seaward transport of sediment following a glacial lake outburst flood and discuss wider implications for sediment transport, geohazards, and insights into the depositional records in marine settings.

2. Geographic Setting

Bute Inlet is a 74 km-long fjord in the Pacific Ranges of the Coast Mountains of British Columbia, Canada (Figure 1). Mountains exceeding 3,000 m above sea level are common within the watershed, and many host small

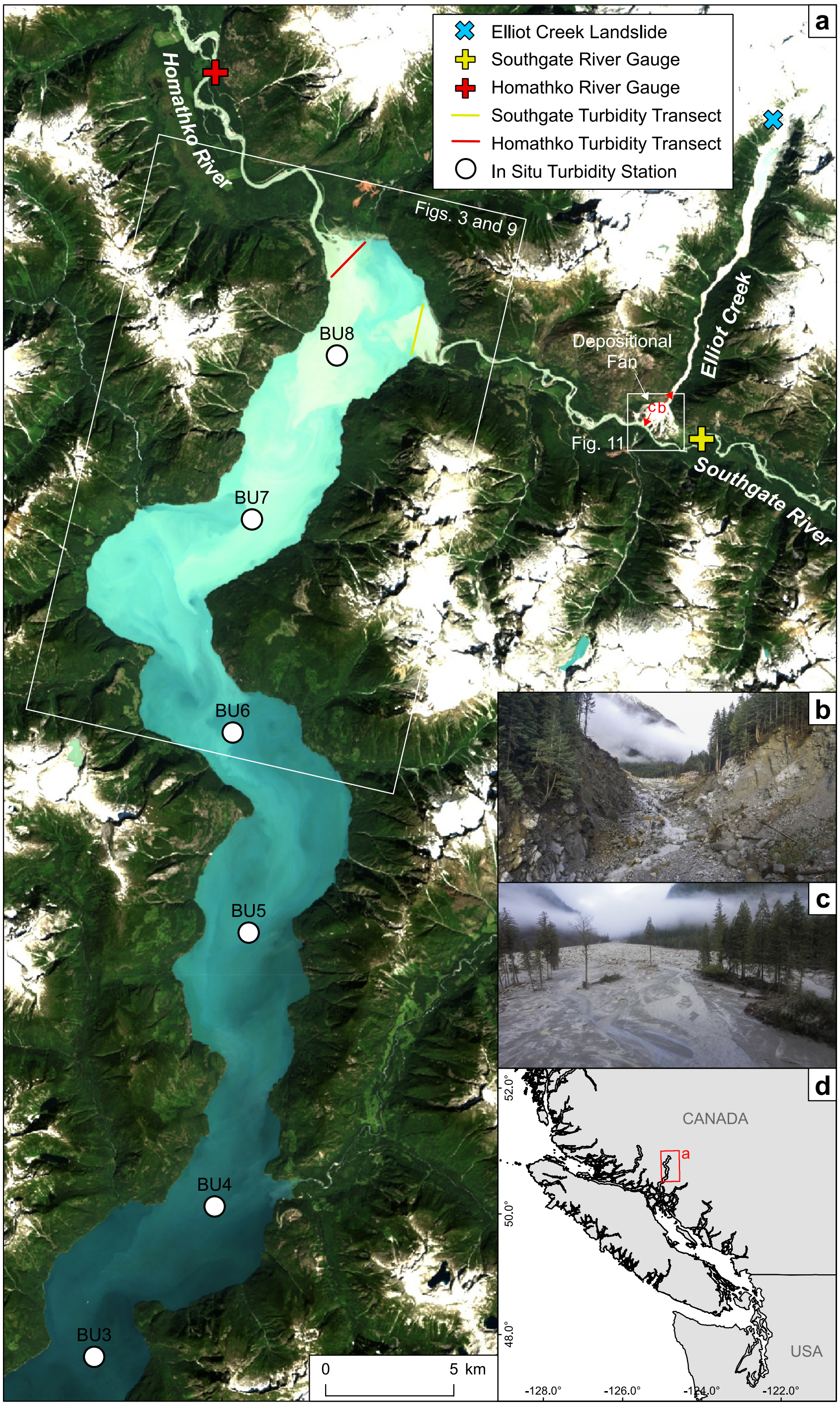

Figure 1. Location map of Bute Inlet and Elliot Creek, British Columbia, Canada. (a) Acolite corrected Landsat 8 OLI scene from 30 July 2021 showing Bute Inlet and the depositional fan formed at the confluence of Elliot Creek with the Southgate River. The locations of the Homathko and Southgate river gauges, in situ turbidity measurements, and transects used for collecting satellite-derived turbidity measurements are also shown. Aerial photographs of (b) erosion in Elliot Creek (source: Kat Pyne, Hakai Institute) and (c) the depositional fan at the confluence of Elliot Creek and the Southgate River (source: Grant Callegari, Hakai Institute) following the 28 November 2020 outburst flood. Locations and facing directions of (b) and (d) shown in panel (a). (d) Map to show the location of Bute Inlet on the west coast of Canada.

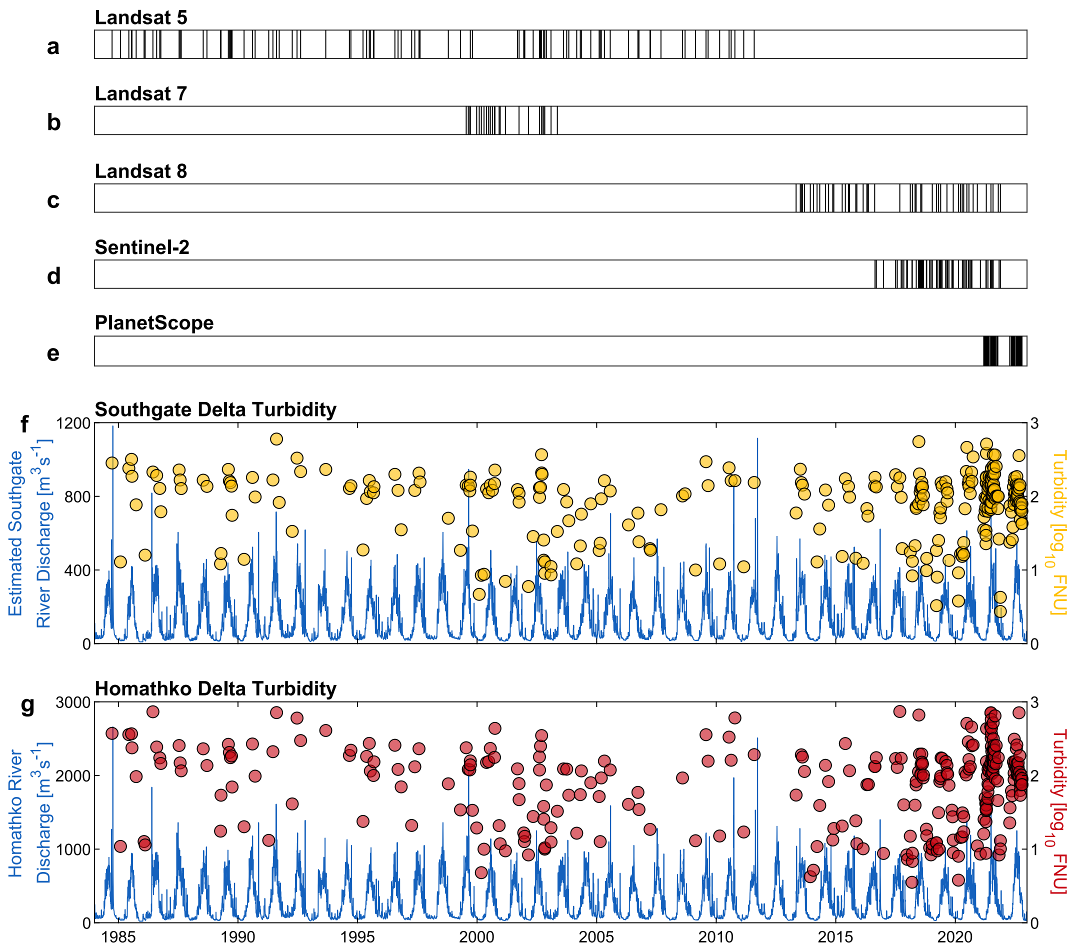

Figure 2. Time series overview of satellite images acquired with river discharge measurements between 1984 and 2022. Dates of (a) Landsat 5, (b) Landsat 7, (c) Landsat 8, (d) Sentinel-2, and (e) PlanetScope images acquired. Maximum satellite derived turbidity estimated using the Acolite code from transects offshore the (f) Southgate River delta with estimates of Southgate River discharge for comparison and (g) Homathko River delta with Homathko River discharge observations for comparison.

ice caps and valley glaciers; however, no previous outburst flood activity has been documented. The Southgate and Homathko rivers, which enter at the head of Bute Inlet (Figure 1a), drain watershed areas of 1,985 and 5,782 km^2, respectively; the Southgate River has a greater area of glacier cover (33.5% compared to 19.1%; Giesbrecht et al., 2022). Both rivers display a typical nival regime; low flows are observed in the winter when water is stored in the seasonal snowpack, followed by high flows during the snowmelt-driven freshet in spring and early summer and periods of convective activity in the late summer (e.g., Déry et al., 2005, 2016). The Homathko River has an average discharge of 250 m^{3}s^{-1}, but often exceeds daily discharge maxima of 1,000 m^{3}s^{-1} during the May to August freshet season and decreases to 50 m^{3}s^{-1} in January to February (Water Survey of Canada station 08GD004; Figure 1a). Sharp peaks in discharge often occur in late October to November, following periods of intense rainfall (sometimes in excess of 2,000 m^{3}s^{-1}). The Southgate River has been gauged since June 2021 (as a result of the 2020 Elliott Creek outburst flood), with discharge measurements of approximately half of the Homathko River (Water Survey of Canada station 08GD010; Figure 1a; Hage et al., 2022).

Fjord surface turbidity correlates with river discharge, with more turbid surface waters observed at the fjord head and decreasing to the mouth of the inlet (e.g., Pickard & Giovando, 1960). Estimates of maximum suspended sediment concentrations for the Homathko River are 0.5–0.7 kg m^{-3}, which are insufficient for plunging of (hyperpycnal) river floodwater (Bornhold et al., 1994; Mulder & Syvitski, 1995). However, frequent (tens per year) turbidity currents can initiate from surface sediment plumes at the Homathko Delta and flow down-slope through the submarine channel (e.g., Bailey et al., 2023; Bornhold et al., 1994; Hage et al., 2019; Pope

Table 1
Details of Satellite Imagery Data Used for Remote Sensing and Estimates of Sea Surface Turbidity in Bute Inlet

Satellite	Imager	Scenes [n]	Resolution [m]	Coverage
Landsat 5	Thematic Mapper	95	30	1984–2011
Landsat 7	Enhanced Thematic Mapper Plus	27	30	1999–2003
Landsat 8	Operational Land Imager	50	30	2013–2021
Sentinel-2	Multi-Spectral Instrument	63	10	2016–2021
PlanetScope	Classic Dove/Dove-2/SuperDove	85	3	2021–2022

et al., 2022). This submarine channel extends from the deltas of the Homathko and Southgate rivers for ∼40 km down-fjord to end at a water depth of 660 m (Figure 1a; Conway et al., 2012; Heijnen et al., 2020).

3. Methods

3.1. River Discharge, Water Level and Meteorological Monitoring

Daily river discharge data were obtained from the Homathko River between 1984 and 2022 (Water Survey of Canada stations 08GD004; Figure 2g), and for the Southgate River from June 2021 to 2022 (Water Survey of Canada station 08GD010; Figure 1a; https://wateroffice.ec.gc.ca). Prior to gauge installation, estimates of Southgate River discharge were assumed to be 44.5% of the discharge recorded at the Homathko River station. This value (of 44.5%) is the difference between the mean Southgate River and the mean Homathko River discharge since gauge installation on the Southgate River (Figure 2f). Water level estimates were calculated using tidal predictions for peak high and low tides at Orford Bay (Figure 1a; https://tides.gc.ca). A time series of tidal heights was produced by fitting a cubic interpolation to splice these tidal data into hourly measurements.

3.2. Satellite Data Acquisition, Correction, and Sea Surface Turbidity Estimates

Turbidity refers to the "cloudiness" of water caused by particles, which has a strong correlation with total suspended material. Sea surface turbidity in Bute Inlet was investigated using a data set of 320 optical satellite images acquired between 1984 and 2022 (Figures 2a–2e). These include scenes with minimal (<40%) cloud coverage over Bute Inlet that were acquired from Landsat 5, 7, and 8, Sentinel-2, and PlanetScope satellites (Table 1). Top of atmosphere images (i.e., reflectance values including contributions from clouds, atmospheric aerosols and gases in addition to the surface) were downloaded from the United States Geological Survey Earth Explorer (Landsat; https://earthexplorer.usgs.gov), the Copernicus Open Access Hub (Sentinel-2; https://scihub.copernicus.eu), and the Planet Explorer (PlanetScope; https://www.planet.com/explorer).

Sea surface turbidity estimates were determined using the open access Acolite code (https://odnature.naturalsciences.be/remsem/software-and-data/acolite; Vanhellemont & Ruddick, 2014, 2018). Top of atmosphere images were first corrected for atmospheric effects using red and near infrared channels using an automated image-based "dark spectrum fitting" approach (Vanhellemont, 2019a, 2019b, 2020; Vanhellemont & Ruddick, 2018) to retrieve water-leaving radiance reflectance in the red band. Sea surface turbidity was then calculated for each colour pixel (e.g., Figures 3a and 3b) from the water leaving reflectance. In optical terms, this turbidity estimate is the measurement at 860 nm (near infrared) of the ratio of 90°-scattered light to forward-transmitted light as compared to the same ratio for a suspension of Formazin ($C_2H_4N_2$). Using this definition, turbidity is measured in Formazin Nephelometric Units (FNU; Nechad et al., 2009) such that

$$T = \frac{A\rho_w}{1 - \rho_w/C}$$

Where ρ_w is the water-leaving reflectance, and A and C are the calibration coefficients. These coefficients are derived by Nechad et al. (2009) and are based on correlations between the wavelength of the red band of satellite images and in situ surface water turbidity measurements. The *A* and *C* coefficients have been further calibrated in the Acolite code specifically for Landsat 8 and Sentinel-2. Landsat 8 red band values for 654 nm were used: $A = 346.32$ gm^{-3} and $C = 0.19905$; and the Sentinel-2 red band values at 655 nm were used: $A = 342.10$ gm^{-3} and

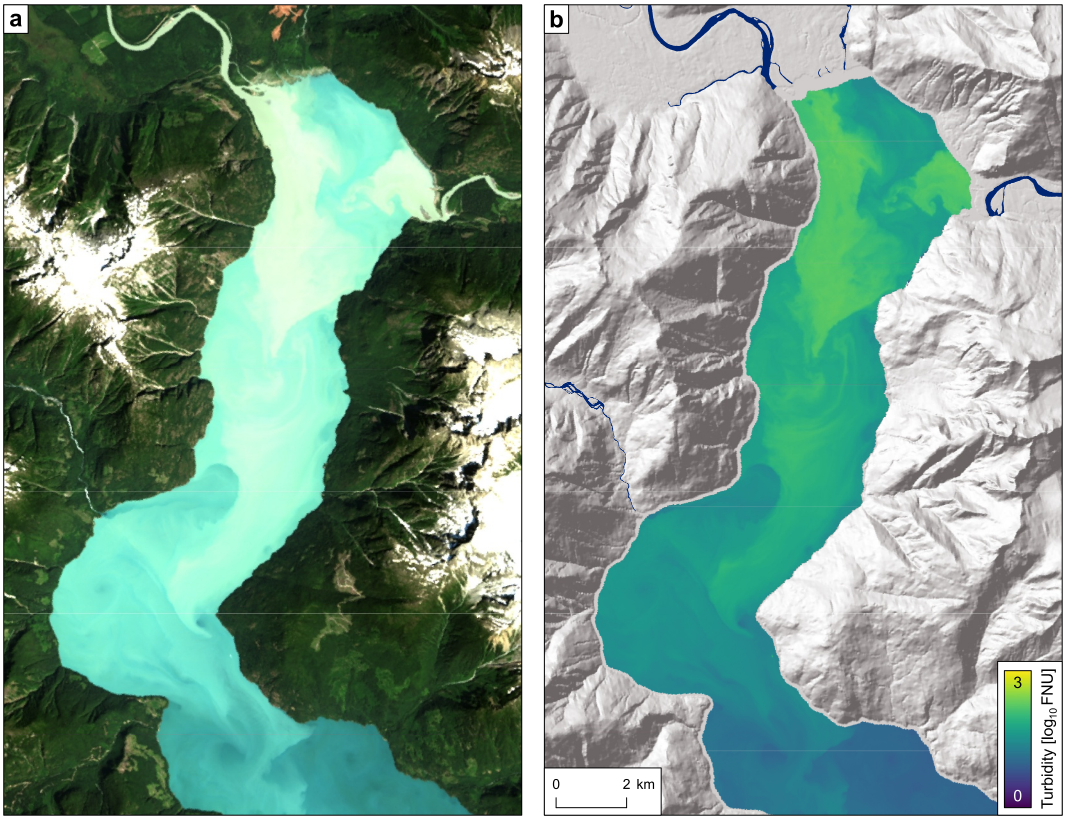

Figure 3. Example of a colour satellite image converted to sea surface turbidity using a Landsat 8 OLI scene from 30 July 2021. (a) Acolite corrected image. (b) Estimates of sea surface turbidity using pixel colour and the algorithm of Nechad et al. (2009) with land areas removed. The spatial extent of each image is shown in Figure 1a.

$C = 0.19563$. All satellite images were converted to 30 m resolution (for consistency between different satellites) before turbidity point measurements were extracted from two transects with 100 m point spacing offshore of the Homathko and Southgate Deltas (Figure 1a). Satellite-derived turbidity measurements have previously been shown to correlate well with in situ measurements in other locations (Vanhellemont, 2019a, 2019b) and showed comparable results for scenes obtained on the same day between different satellites at Bute Inlet (Figure 4).

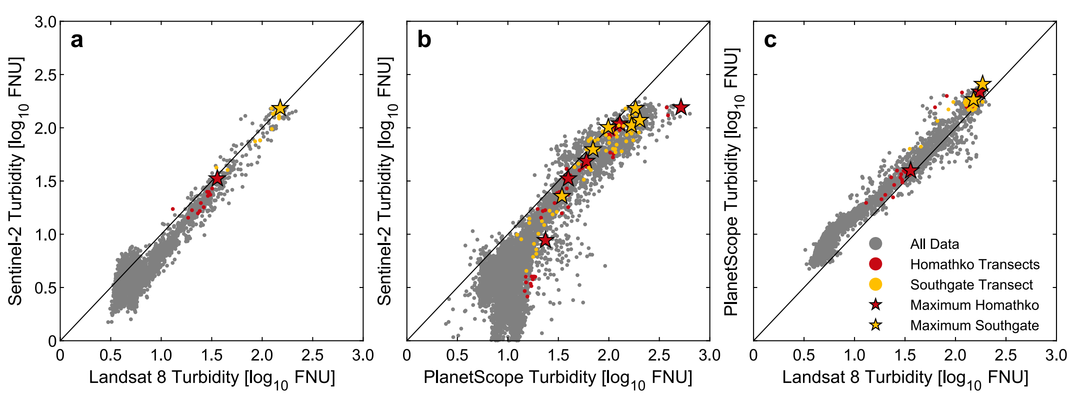

Figure 4. Comparison of estimated turbidity measurements captured on the same day by different satellites. Cross plots show data from (a) Landsat 8 against Sentinel-2 ($n = 1$); (b) PlanetScope against Sentinel-2 ($n = 5$); and (c) Landsat 8 against PlanetScope ($n = 2$). Each plot shows the comparison between all data from scenes of the same date and the transect offshore the Homathko and Southgate Deltas, with maximum turbidity measurements highlighted.

3.3. In Situ Near Surface Turbidity Measurements

Water column profiles of in situ turbidity measurements were recorded at eight stations along Bute Inlet (Figure 1a) over 42 days between 2018 and 2022 (with sampling intervals varying between 2 and 18 weeks). Data were collected using Seapoint Turbidity meters attached to conductivity, temperature and depth (CTD) profilers. Seapoint turbidity meters have a near-infrared light source (880 nm) and were factory calibrated with Formazin to quantify turbidity in Formazin Turbidity Units (FTU). Measurements were rated to have a linear response (±2%) to particle concentrations spanning 0–1250 FTU. Profile data were binned into 1 m depth intervals from the surface to just above the seafloor. In this study, we show only turbidity measurements between 2 and 5 m water depth from the six most delta-proximal stations (labelled BU3-8 in Figure 1a). Turbidity measurements recorded at water depths shallower than 2 m were omitted due to interference with bubbles from the vessel propeller. In situ measurements of turbidity are compared with satellite-derived estimates of turbidity. The difference in units between satellite-derived turbidity estimates (Formazin Nephelometric Units) and in situ measurements (Formazin Turbidity Units) relate to the methods of data collection, with values remaining comparable.

4. Results

4.1. Background Seasonal Variations in Sea Surface Turbidity in Bute Inlet

Sea surface sediment plumes were visible offshore from both the Homathko and Southgate rivers between May and October in all 218 satellite images between 1984 and 28 November 2020 (i.e., date of the Elliot Creek outburst flood). Prior to the glacial lake outburst flood, higher values of sea surface turbidity across the entire fjord closely track the discharge from the Homathko and Southgate rivers (Figure 5). For example, both satellite-derived and in situ turbidity measurements showed an annual cycle resembling the hydrograph of the Homathko River with the highest turbidity values observed during the freshet season (Figures 6 and 7). Nearshore sea surface turbidity generally increased to a threshold of between ~2.5 and 3.0 $\log_{10}$ FNU during the freshet period of elevated river discharge (May to August). During the winter (when river discharge is low), near-delta turbidity was typically <1.5 $\log_{10}$ FNU (Figures 5–7). However, a disconnect between sea surface turbidity and river discharge was observed on the rising and falling limbs of the freshet season. For example, from 1984 to the 2020 outburst flood, the month with the highest median Homathko River discharge was July (Figure 6a). However, the highest sea surface turbidity measurements for both the Southgate and Homathko rivers occurred in June on the rising limb of river discharge (Figures 6b and 6c).

4.2. Sea Surface Turbidity Immediately After the Elliot Lake Outburst Flood

Turbid water could be observed in satellite images of Bute Inlet for the 3 months directly following the glacial lake outburst flood; however, shadowing or cloud coverage meant quantification of sea surface turbidity directly offshore the Southgate Delta was not possible. However, during this period, in situ turbidity measurements in Bute Inlet were recorded at a series of CTD profiler stations (Figure 1a), including 4 and 16 days following the glacial lake outburst flood in Elliot Creek (Figures 8b and 8c). Temporal data coverage was low relative to the resolution of spring/summer satellite images. However, in situ near sea surface (2–5 m water depth) measurements showed increased turbidity at the head of Bute Inlet following the 28 November 2020 event. Despite this increase, measured changes in sea surface turbidity during the initial 3 months following the outburst flood were within the range of measurements observed before the event at the most delta-proximal station (BU8; Figure 7d). Furthermore, the initial (4 and 16 days) post-outburst flood turbidity measurements were 2–3 times lower in the upper reaches of the fjord (stations BU5-8; Figure 1a) than observations prior to the outburst flood event during the end of the 2020 freshet season (22 October 2020; Figure 8).

4.3. Delayed Response in Fjord-Surface Turbidity Following the Outburst Flood

The first cloud- and shadow-free satellite image (10 March 2021) following the Elliot Lake outburst flood reveals a surface sediment plume offshore from the Southgate River, and not the Homathko River. This is notable as the Homathko River usually dominates the sediment supply to the fjord (Figures 7a and 7b). The satellite-derived surface turbidity offshore the Southgate River was anomalously high compared to the same time of year for all pre-outburst flood measurements (Figure 7a). The surface sediment plume offshore from the Southgate River remained visible through March and into April 2021. The plume rapidly increased in turbidity magnitude and down-fjord extent between 16 and 18 April 2021 when turbidity rose dramatically (Figures 9d and 10), eventually

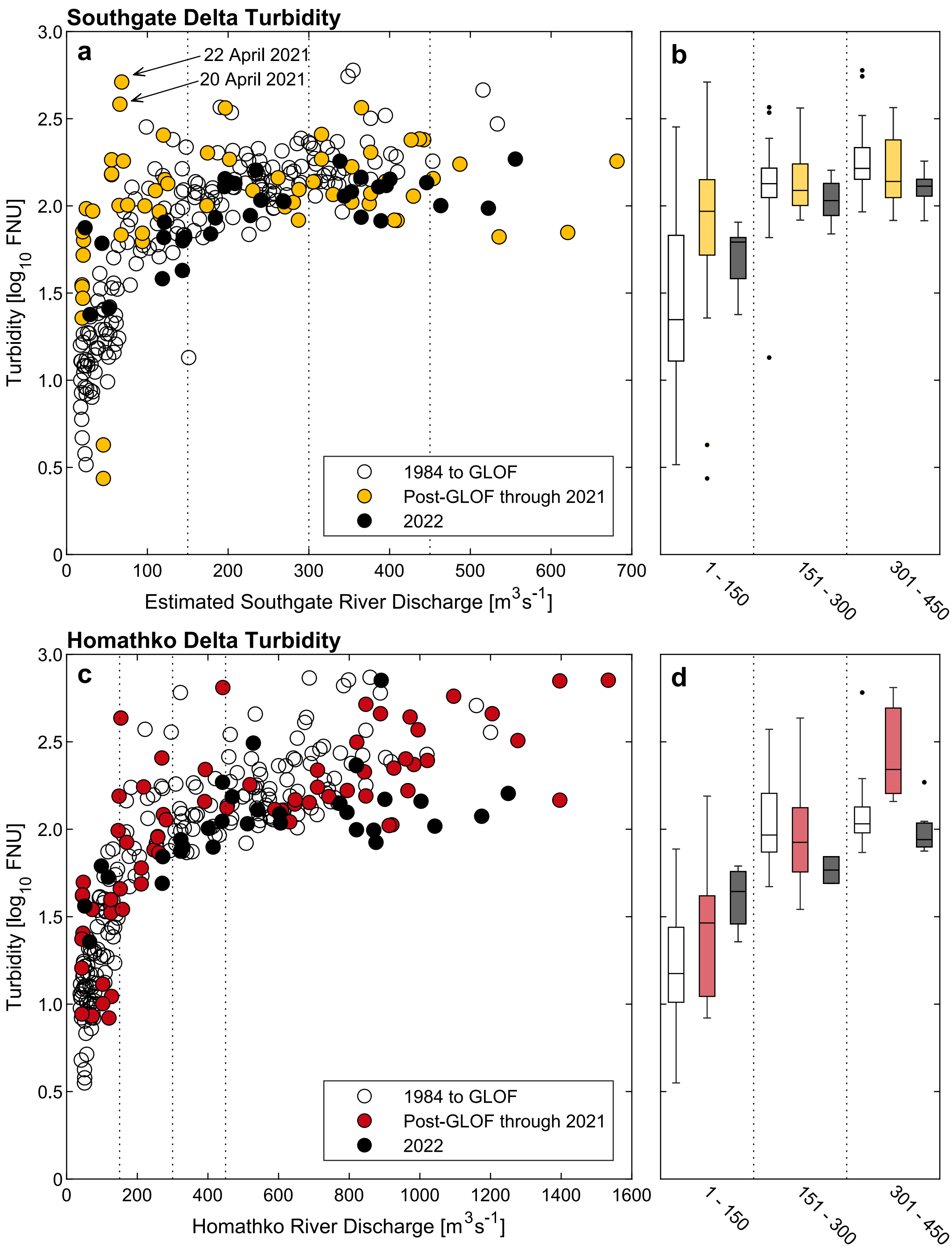

Figure 5. Comparison between river discharge and nearshore sea surface satellite-derived turbidity measurements. Data points in all plots are coloured to show timing pre-glacial lake outburst flood (GLOF), post-GLOF through 2021 or during 2022. (a) Cross plot showing variation of nearshore sea surface turbidity estimates offshore the Southgate River delta with Southgate River discharge estimates (taken as 44.5% of Homathko River discharge). (b) Distribution of turbidity for binned intervals of Southgate River discharge estimates. (c) Cross showing variation of nearshore sea surface turbidity estimates offshore the Homathko River delta with Homathko River discharge. (d) Distribution of turbidity for binned intervals of Homathko River discharge.

peaking on 20 and 22 April 2021 (Figures 7a and 10). The highest satellite-derived turbidity values (2.6 and 2.7 $\log_{10}$ FNU) thus occurred almost 5 months after the initial outburst flood. These peak turbidity values were more than double the median values for April and are within the top 2% of all turbidity observations from the 1984–

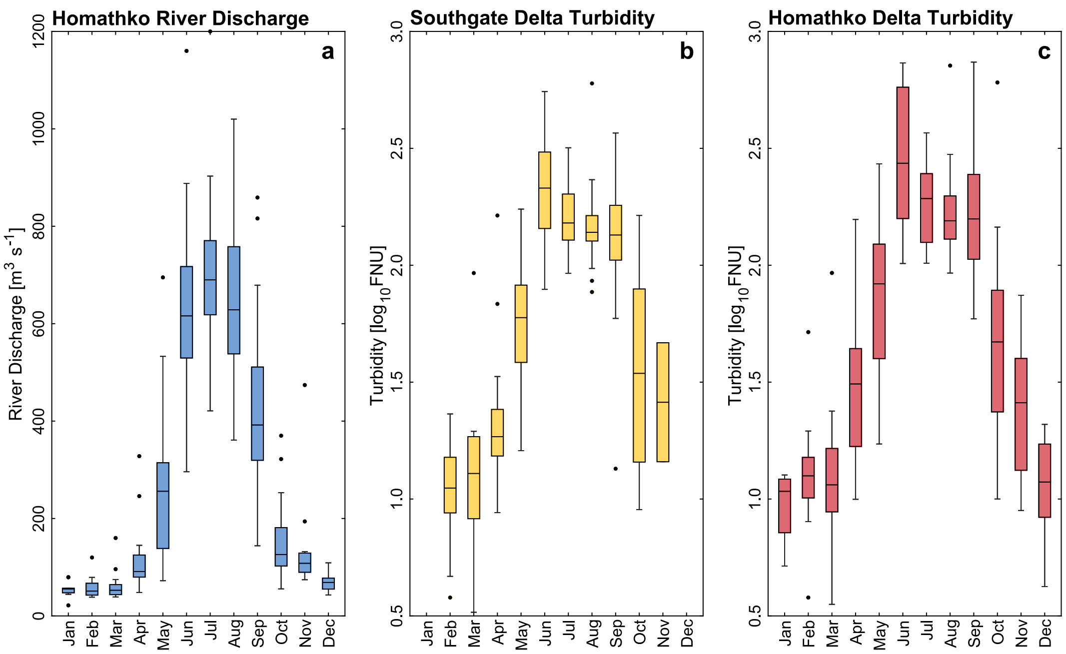

Figure 6. Box and whisker plots to show annual hydrographic and satellite-derived turbidity cycles in Bute Inlet. Box and whiskers represent monthly data between 1984 and 2022 of sea surface turbidity from transects in Figure 1a offshore (a) the Southgate River delta and (b) the Homathko River delta along with (c) discharge from the Homathko River.

2022 data set (Figures 3a, 5a and 7a). Following a week-long (16–22 April 2021) increase in turbidity, cloud cover obscured satellite images, inhibiting surface turbidity analysis until 4 May 2021 (Figure 10). After this, the satellite-derived turbidity in the upper fjord resembled pre-outburst flood observations throughout the remainder of the 2021 freshet (despite increasing river discharge), and the entirety of 2022 (Figures 7a and 9).

The elevated post-outburst flood sea surface turbidity (Figures 7a and 9d) cannot be attributed to higher-than-expected river discharge (Figure 5a), and no correlation between tidal changes in water level and turbidity was observed. In fact, the only significant differences in pre-to post-outburst flood sea surface turbidity (i.e., median turbidity value outside the interquartile range) were observed for Southgate River discharges below 150 m^3s^{-1} (Figure 5b). Remarkably, the period of high turbidity between 16–22 April 2021 occurred when the Southgate River discharge was only ~65 m^3s^{-1}, yet peak turbidity values were five times higher than pre-outburst flood measurements for the same Southgate River discharge (Figure 5a). The Southgate River discharge at this time was thus very low compared to a peak discharge of ~1,000 m^3s^{-1} during the 2021 freshet (Figures 5a and 10), but the turbidity increase did align with the first, albeit minor, increase in river discharge at the onset of the freshet (Figure 10). The timing of this turbidity increase also aligned with the first instance of water sourced from Elliot Creek breaching the depositional fan and entering the Southgate River (Figure 11). It is not possible to quantify the volume of water flowing through Elliot Creek; however, it would have been minor in comparison to Southgate River discharge. High sea surface turbidity at the onset of the freshet season was mostly confined proximal to the Southgate Delta. In situ turbidity measurements from BU8 (located ~4 km from the fjord head; Figure 1a) showed no obvious variation between pre- and post-outburst flood measurements for March and April, despite showing minor elevations during the winter (Figure 5d). A surface sediment plume offshore from the Homathko Delta is first visible on 16 April, 2021. However, the surface turbidity offshore the Southgate Delta on this date was higher than that offshore the Homathko Delta (Figure 7c). Satellite-derived turbidity offshore the Homathko Delta did show a peak of turbidity between 26 June and 6 July 2021, which was not observed offshore the Southgate Delta (Figure 5). This turbidity peak occurred when the Homathko River discharge was >1,600 m^3s^{-1}, the highest river discharge recorded during the freshet season for 22 years (Figure 2g) that coincided with the 2021 Heat Dome, in which British Columbia experienced record temperatures (Philip et al., 2022). As such, while the turbidity recorded during the Heat Dome was elevated, the values are consistent with previous measurements obtained for similar Homathko River discharges (Figure 5c).

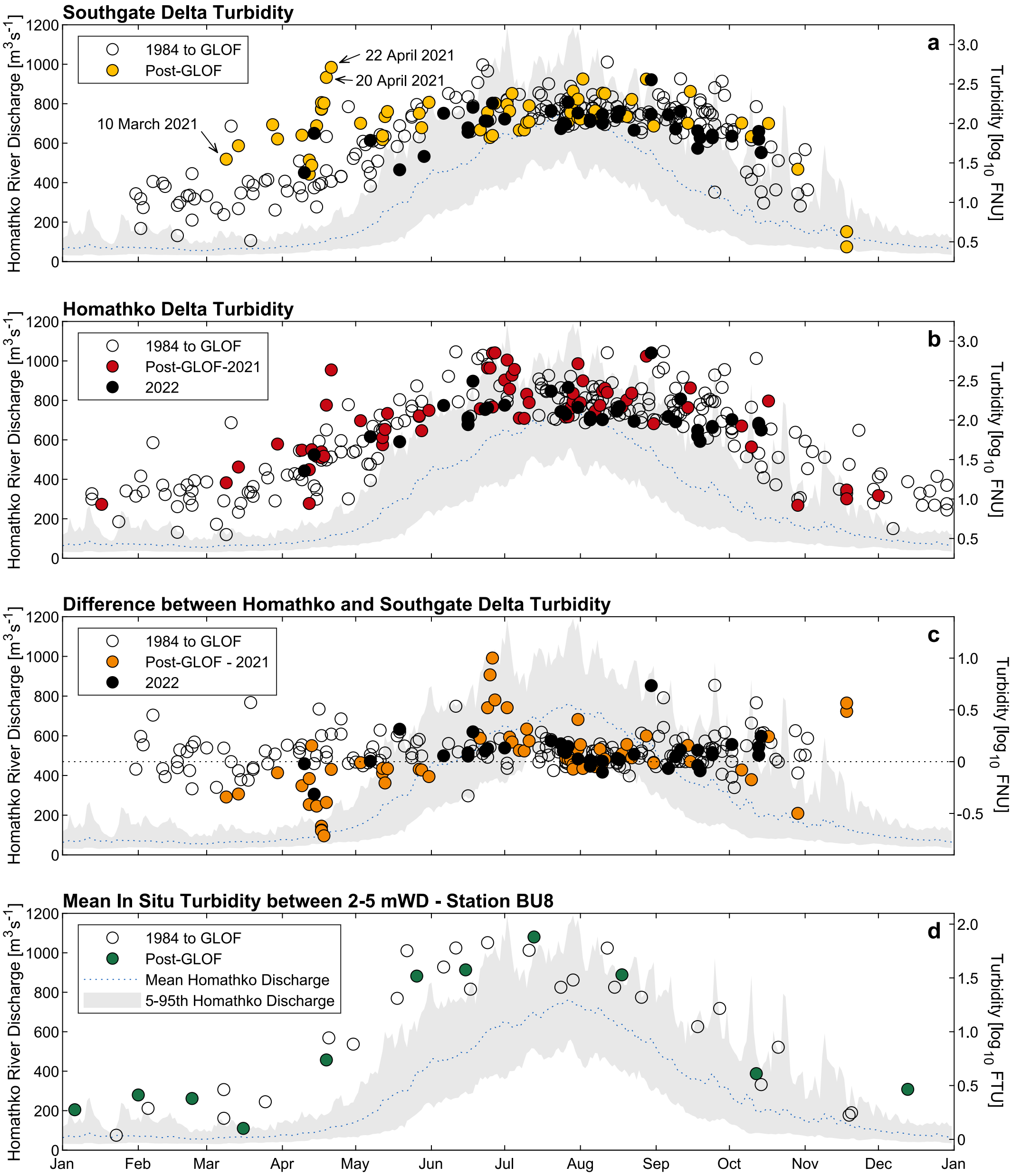

Figure 7. Day-of-year time series of turbidity measurements recorded between 1984 and 2022. Using the transects shown in Figure 1a. (a) shows satellite-derived sea surface turbidity offshore the Southgate River delta and (b) offshore the Homathko River Delta. (c) The difference between turbidity measurements recorded offshore the Homathko and Southgate River deltas. (d) In-situ turbidity recorded at station BU8 (Figure 1a) averaged between 2 and 5 m water depth. Data points are colored depending on timing relative to the glacial lake outburst flood. All panels show the mean 5–95th percentile range of daily Homathko River discharge between 1984 and 2022.

5. Discussion

5.1. Controls on Sea Surface Turbidity at the Head of Bute Inlet

Here we discuss how sediment supply, regulated by river discharge, is the dominant control on background sea surface turbidity proximal to the Homathko and Southgate Deltas. A close relationship exists between fjord-head surface turbidity and discharge from the Homathko and Southgate rivers (Figure 5). For example, elevations in river discharge result in an increase in sea surface turbidity up to a value of ~2.5 $\log_{10}$ FNU, which equates to a sediment concentration of ~1 kg m^{-3}. Sediment in the surface sediment plume then has the potential to plunge or

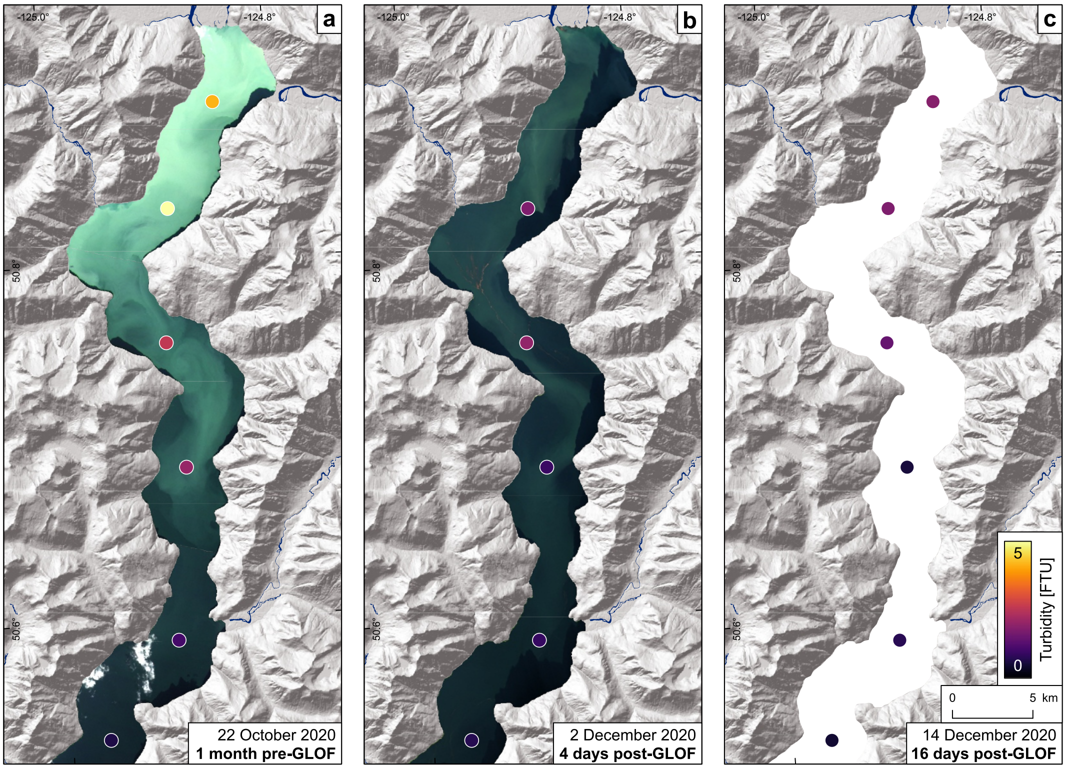

Figure 8. In-situ near-sea surface (averaged between 2 and 5 m) turbidity measurements in Bute Inlet pre- and post-outburst flood on (a) 22 October 2020 (with Acolite corrected PlanetScope scene clipped to water pixels from 21 October 2020), (b) 2 December 2020 (with Acolite corrected Landsat 8 scene from the same day; NB. no data collected at station BU8); and (c) 14 December 2020 (no cloud free satellite scene was available within 2 days of this date).

settle out of suspension (e.g., Hoyal et al., 1999; Parsons et al., 2001). Seasonal variations in nearshore sea surface turbidity should therefore be expected to follow the hydrographs of the Homathko and Southgate rivers (Pickard & Giovando, 1960). As such, turbidity should remain low from January to April, increase through the start of the freshet season and peak in July and August, before decreasing for the remainder of the year—aside from occasional peaks in rainfall-induced river discharge. However, sediment flux does not increase linearly with river discharge (e.g., Hickin, 1989). Our analysis demonstrates this, with peak nearshore turbidity preceding peak freshet season river discharge (Figure 6). This hysteresis between turbidity and the rising and falling limbs of freshet river discharge can be attributed to greater sediment availability at the start of the freshet season (i.e., the "first-flush"; Riihimaki et al., 2005). For example, during the winter, large volumes of sediment accumulate in the river channel and at the mouth bars at the top of the Homathko and Southgate Deltas (or indeed other seasonally fed bedload dominated rivers; e.g. Wright, 1977). Elevations in river discharge on the rising limb of the freshet season are sufficient to resuspend and flush delta-top sediment. Depletion of sediment in the Southgate and Homathko rivers and delta-tops during the falling limb then generates the hysteresis loop observed in fjord-head turbidity. This process allows surface sediment plumes to form offshore from both the Homathko and Southgate rivers at relatively low (<150 $m^3 s^{-1}$) discharge at the start of the freshet season (e.g., Figure 9).

5.2. Did Sea Surface Turbidity Increase Immediately Following the Outburst Flood?

During the 28 November 2020 Elliot Lake outburst flood, ~4.3×10^6 m^3 of sediment was directly transported into the marine environment of Bute Inlet (Geertsema et al., 2022). While it is almost certain that a pronounced sea-surface sediment plume was present in Bute Inlet during the Elliot Creek outburst flood, no usable satellite imagery or in situ CTD data could be found to confirm this. While minor increases in near-surface turbidity were observed in the 3 months following the outburst flood, these were within the range of measurements observed prior to the event (Figures 7 and 8). Conversely, in situ turbidity below a water depth of 200 m showed a fivefold

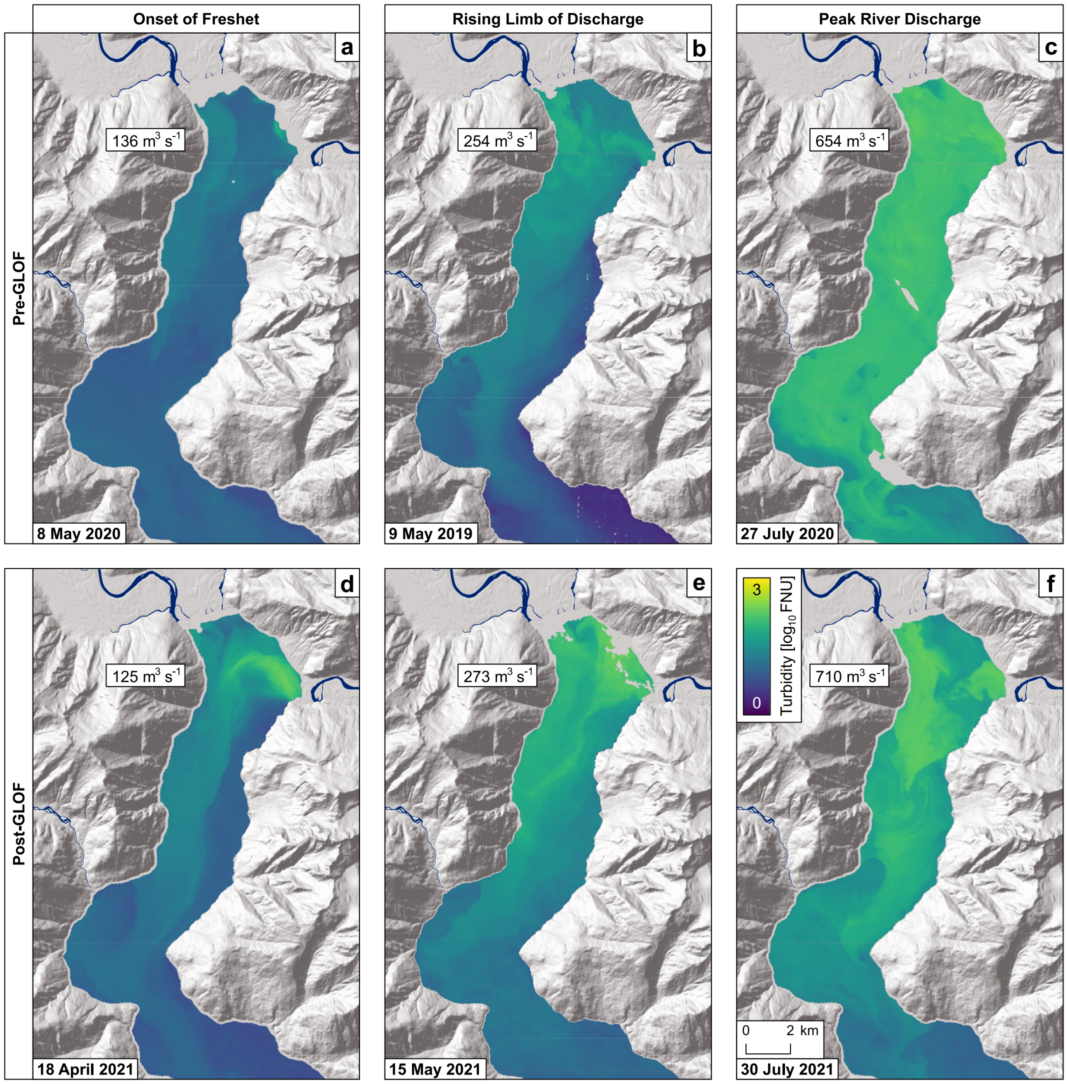

Figure 9. Satellite-derived estimates of sea surface turbidity in upper Bute Inlet at different periods in the freshet season pre- and post-outburst flood. Turbidity estimates convert colour images from (a) Landsat 8 from 8th May 2020; (b) Sentinel-2 from 9th May 2019; (c) Landsat 8 from 27th July 2020; (d) Landsat 8 from 8th May 2021; (e) PlanetScope from 15th May 2021; and (f) Landsat 8 from 30th July 2021. Each panel includes the daily average discharge from the Homathko River for the corresponding day. Estimates are calculated using the algorithm of Nechad et al. (2009) in the Acolite code. The spatial extent of each image is shown in Figure 1a.

increase throughout the upper 60 km of Bute Inlet (Geertsema et al., 2022). The potential absence of an initial distinct surface sediment plume following the outburst flood could be attributed to hyperpycnal plunging of sediment as it entered the fjord. The relative increase in surface turbidity during the 2020/21 winter, which followed the outburst flood, compared to previous years likely represents finer sediment from the outburst event remaining in suspension (Figure 7d).

5.3. Explanations for the Sea Surface Turbidity Response Following the Outburst Flood

While a minor increase in nearshore surface turbidity was observed following the Elliot Lake outburst flood (Figure 7d), the greatest disparity between pre- and post-outburst flood turbidity was observed almost half a year later. Five months after the Elliot Lake outburst flood, relative turbidity peaked to exceptional levels offshore from the Southgate River at the onset of the 2021 freshet season (Figures 7a and 10). Sea surface turbidity values

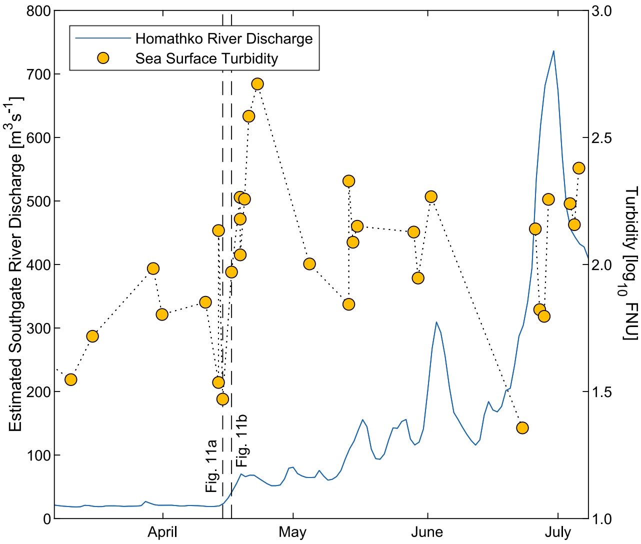

Figure 10. Estimated Southgate River discharge and satellite-derived estimates of sea surface turbidity offshore the Southgate River delta at the start of the 2021 freshet season. Vertical lines denote the dates of images of the Elliot Creek depositional fan shown in Figure 11.

at this time were in the top 2% of all measurements from 1984 to 2022 (Figures 2f and 5a). We explore two mechanisms that could individually or together explain this anomalous turbidity peak in April 2021 (Figure 12).

The first mechanism is an upscaled version of the hysteresis effect observed during a typical annual cycle (Figure 6), whereby sediment is transported to and deposited at the delta during the winter (e.g., Wright, 1977). We suggest that eroded material from the glacial lake outburst flood results in an increased volume of Southgate River channel sediment below the confluence with Elliot Creek (Figure 1a; c.f. Geertsema et al., 2022). Thus, a much greater volume of sediment was likely transported to the Southgate Delta during the 2020/21 winter in comparison to previous years. The 5-month lag period from the initial outburst flood to the inception of surface sediment plumes offshore the Southgate Delta is likely due to insufficient bed shear stresses during the low winter river discharge, which were incapable of mobilising and flushing sediment. It was only at the onset of the 2021 freshet, when the Southgate River discharge increased sufficiently, that bed shear stresses reached a critical threshold to remobilise delta sediments emplaced during the outburst flood. Such flushing of sediment is demonstrated by the week-long period (16–22 April 2021) of elevated sea surface turbidity offshore the Southgate Delta (Figure 10). The observation of a short-lived pulse of elevated sea surface turbidity provides further evidence of an upscaled hysteresis effect. For example, the reduction in sea surface turbidity following 22 April 2021 (Figure 10) likely marks the time when excess sediment availability on the delta-top was exhausted. Here, the surface sediment plume offshore the Southgate River more closely resembles pre-outburst flood observations (Figures 7a and 9).

The second potential mechanism relates to the emplacement of a 2 km^2 depositional fan at the confluence of Elliot Creek and the Southgate River (Figures 1a and 1c; see Figure 1 in Geertsema et al., 2022). While this sediment load was deposited during the outburst flood, the low water level of the Southgate River during winter (once flood waters had subsided) would have limited remobilisation and transportation downstream. Increased Southgate River discharge at the onset of the freshet season (e.g., Figure 10) would increase both the height of the water line and stream power. This combination would likely have eroded material previously above the water line during the

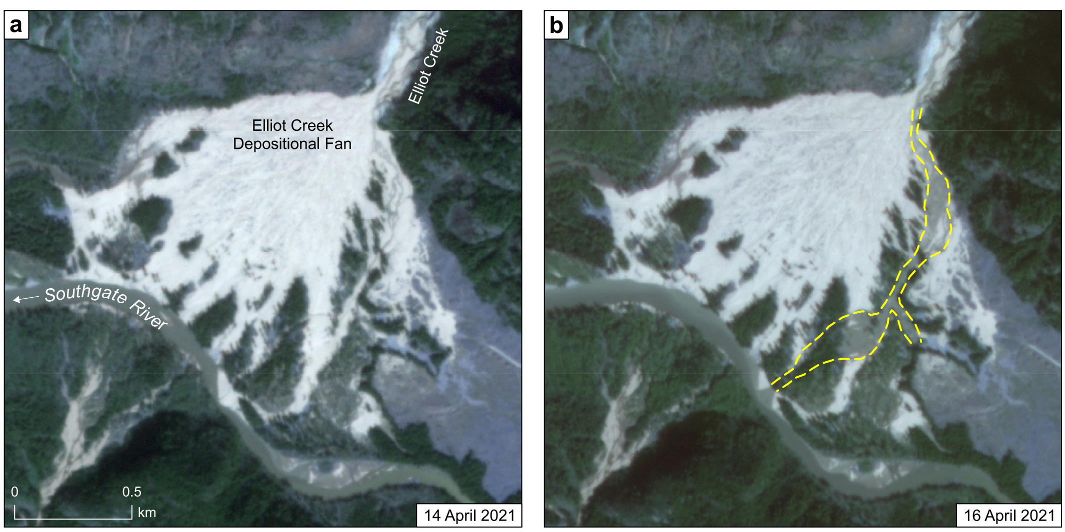

Figure 11. Satellite images showing first visible water flow across the Elliot Creek depositional fan in 2021. Acolite corrected PlanetScope (3 m resolution) images from (a) 14 April 2021 and (b) 16 April 2021. Area within yellow dashed lines in panel (b) shows water flow over the Elliot Creek depositional fan. No water flow is visible for the same area in panel (a).

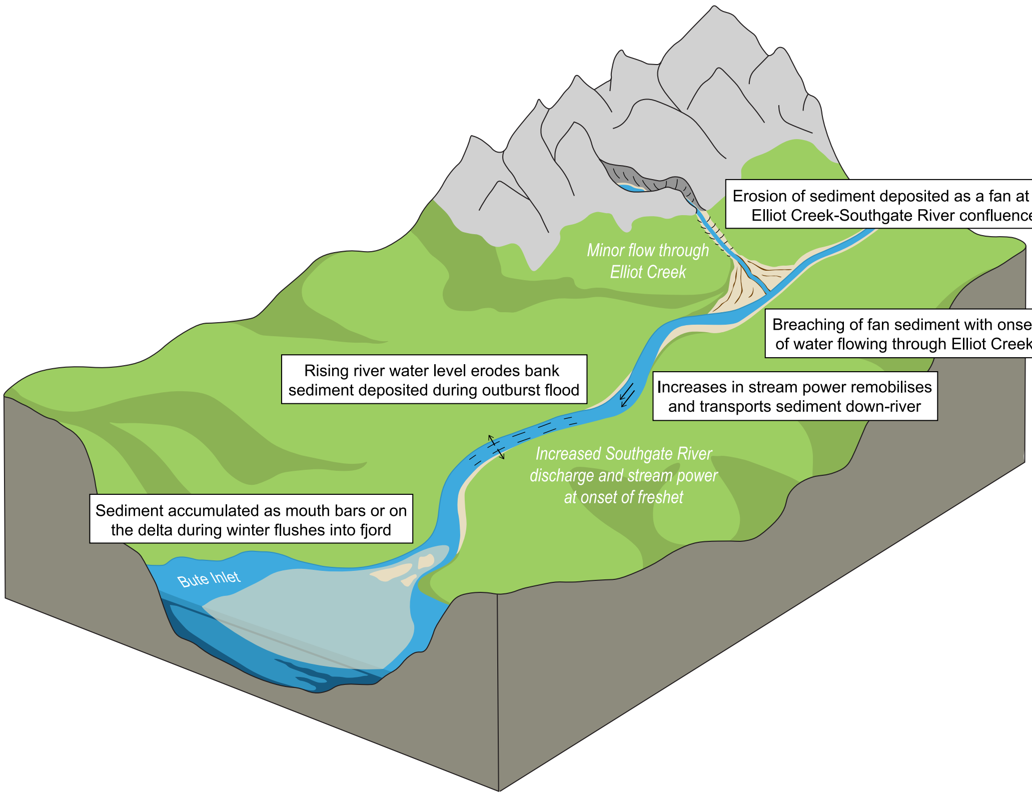

Figure 12. Schematic to show sediment transport mechanisms following the Elliot Lake outburst flood leading to the generation of a lagged response in elevated sea surface turbidity.

winter, as well as coarser sediment, which was then transported to the Southgate Delta and flushed offshore, therefore increasing fjord-head turbidity. Additionally, increased flow of meltwater from Elliot Lake through Elliot Creek provides an additional mechanism to increase sediment concentration in the Southgate River. The volume of water flowing through Elliot Creek is minor compared to the Southgate River. However, peak turbidity recorded in the head of Bute Inlet coincides with the timing of water sourced from Elliot Creek breaching the depositional fan and entering the Southgate River (Figure 11).

The relative peak in sea surface turbidity offshore the Southgate Delta was short-lived, lasting just over a week (Figure 10). Despite continued increases in river discharge (peaking in June), turbidity offshore Southgate Delta resembled pre-outburst flood measurements for the remainder of 2021 and all of 2022 (Figures 7a and 9). We suggest this week-long elevation in sea surface turbidity was due to the availability of excess sediment from the river, either from accumulation during the winter or from the Elliot Creek Fan (Figure 12). The rapid return of turbidity to normal values, resembling pre-outburst flood observations, demonstrates the ability of this system to efficiently flush excess sediment stored in the Southgate River system. This "self-correction" is analogous to traditional (human-made) dam removal on a river. For example, similar short-lived peaks in suspended concentration temporally lag following dam removal until the river discharge also increases (e.g., the Elwha River; Magirl et al., 2015; Ritchie et al., 2018; Warrick et al., 2015).

We infer that the non-freshet timing of the Elliot Lake outburst flood caused the observed 5-month lag between the outburst flood and peak turbidity offshore the Southgate Delta. Had the Elliot Lake landslide and subsequent glacial lake outburst flood occurred during the freshet season, when Southgate River discharge was already elevated, it is likely that sediment would have rapidly been transported and flushed from the Southgate Delta, rather than several months later.

5.4. Implications for a Post-Flood Disconnect of Onshore-to-Offshore Sediment Transport

The lagged sea surface turbidity response offshore from the Southgate Delta signifies a temporal disconnect between the onshore and offshore transport of sediment and other particulate matter following the Elliot Lake outburst flood. It has been suggested that fjord sediments may provide an archive of fjord activity (e.g., Koppes et al., 2015; Koppes & Hallet, 2006), including glacial lake outburst floods (e.g., Piret et al., 2022; Vandekerkhove et al., 2021). However, such a 5 month disconnect between the initial outburst flood, and the transport of associated material in the fjord complicates this link somewhat, most notably in settings with high resolution records (e.g., varved sediment sequences; Xu et al., 2015). Using the case of the Elliot Lake outburst flood as an example, two phases of increased (relative to background conditions) onshore-to-offshore sediment transport were observed. The first sediment transport event occurred during the outburst flood (i.e., the deeper-water sediment plume; Geertsema et al., 2022), with a second sediment transport event occurring 5 months after the outburst flood. While the initial $\sim 4.3 \times 10^6$ m^3 volume of sediment transported to the marine environment of Bute Inlet was likely larger, the second sediment transport event will affect seabed deposits in the fjord. Fine-grained, organic-poor glacial lake outburst deposits that settle from a buoyant plume, and associated turbidity current deposits, have previously been described in fjords (Vandekerkhove et al., 2021). The 5-month difference in transport phases is within the error of high-resolution dating techniques (e.g., radiocarbon or Pb/Cs). However, recognition of reworking is important when considering fjord sediments as geological archives, especially in settings such as Bute Inlet that is known for high turbidity current activity (e.g., Bailey et al., 2023; Bornhold et al., 1994; Pope et al., 2022). Here, it is possible that an outburst flood deposit could be represented by multiple deposits (e.g., Haeussler et al., 2018) or be entirely reworked, especially considering the greater-than-normal sediment supply at the onset of the 2021 freshet further increasing turbidity current activity (e.g., Bailey et al., 2021).

A disconnect between onshore-to-offshore sediment transfer may be applicable to other types of catastrophic water release, in addition to glacial lake outburst floods. One example of a similar sediment transport lag is after the 2015 failure of the Fundão tailings dam in Brazil, when 62×10^6 m^3 of iron mining tailings were released into the Doce River watershed and transported offshore (Carmo et al., 2017; D'Azeredo Orlando et al., 2020; Kütter et al., 2023; Marta-Almeida et al., 2016). An increased number of "high turbidity" events were observed in the Doce River during the next two wet seasons following the accident (Kütter et al., 2023), suggesting that particulate matter was stored and later remobilised. Similar delays between events and offshore transport of sediment, and associated matter, should also be considered where water flows into the marine environment through river systems, following tailing dam collapses (e.g., Islam & Murakami, 2021), jökulhlaups (e.g., Old et al., 2005; Russell et al., 2006; Staines & Carrivick, 2015), volcanic crater or lava-impounded lakes (e.g., Clare et al., 2018) and lahars that reach the ocean or lakes (e.g., Major et al., 2016; Pierson et al., 2013). In all cases, recognising the staging areas and timeframes are important for understanding the oxidation of organic carbon, exposure of ecosystems to pollutants or volcanic ash, and the use of offshore depositional archives to reconstruct past outburst flood events.

5.5. Future Glacial Lake Outburst Floods and Changes to Fjord Environments

It remains unclear whether the frequency of glacial lake outburst floods will increase (Carrivick & Tweed, 2016; Harrison et al., 2018; Vandekerkhove et al., 2020; Veh et al., 2020). However, climate change is rapidly increasing the size and number of glacial lakes (Ahmed et al., 2021; Shugar et al., 2020; Wilson et al., 2018). As such, future lagged transport of outburst flood sediments, and other particulate matter, into the marine environment of fjords could be expected. This is especially likely across the extensive $\sim$70,000 km^2 of glacierised watersheds in the Coast Mountain Range, British Columbia, where streamflow regimes are comparable to Bute Inlet (i.e., low winter flow followed by meltwater freshet in spring; Giesbrecht et al., 2022). Fjords are highly susceptible to environmental change (Marín et al., 2013; Meerhoff et al., 2019), and Bute Inlet has already warmed by 1.3°C and shown an oxygen loss of 0.6 mL L^{-1} since the 1950s in response to global warming (Jackson et al., 2021). Changes in frequency and magnitude through delayed fluxes of particulate matter to fjords will likely lead to further changes in fjord water chemistry and light availability, perhaps irreversibly, impacting marine ecosystems (e.g., Arimitsu et al., 2016; Suchy et al., 2022).

6. Conclusions

As glaciated mountains evolve globally in response to human-exacerbated climate change, the hazards and risks in these landscapes will also evolve. The 28 November 2020 Elliot Creek glacial lake outburst flood immediately delivered ~4.3×10^6 m^3 of sediment into the marine environment of Bute Inlet. While highly likely that a sea surface plume was present during the initial outburst flood (and not observed due to lack of satellite coverage), satellite-derived and in situ measurements show that sea-surface turbidity was surprisingly muted in the initial months after the outburst flood. Only minor surface turbidity increases offshore the Southgate Delta were observed relative to typical elevations recorded during the annual freshet season. Instead, the greatest disparity between pre- and post-flood measurements occurred almost 5 months after the initial Elliot Lake outburst flood. This turbidity peak coincided with the onset of the 2021 freshet season, and was in the top 2% of all measurements recorded from 1984 to 2022. We propose two mechanisms that combine to produce the delayed turbidity peak: (a) sediment accumulates within the river catchment during the winter months when Southgate River discharge is low, and this sediment is subsequently flushed from the delta-top when river discharge increases in the freshet season; and (b) higher river-water levels during the freshet season accessed a larger area of erodible flood-emplaced sediment at the terminus of Elliot Creek. This sediment was then transported to the coast at the Southgate Delta. The short-lived turbidity peak demonstrates the efficiency with which the system can remove excess sediment. The observed lag period between onshore-to-offshore sediment transport at Bute Inlet (and similar lags following other major discharge events) implies that caution should be applied if attempting to directly link offshore deposits with an initial outburst flood. The true picture may be far more complicated than a direct, immediate connection, and requires a holistic understanding of flood initiation, mechanics of onshore transfer, identification of potential storage in staging zones, and of the often-temporally variable processes that ultimately result in the offshore transfer and seafloor accumulation of particulate matter.

Data Availability Statement

The data on which this article is based, including satellite-derived and in situ turbidity data, including dates of images used for satellite comparison, and meteorological data are available in (Bailey et al., 2025) and can be downloaded from https://doi.org/10.5683/SP3/WNRZUD. River discharge data (acquired from Environmental and Natural Resource Canada can be downloaded from the following links; Homathko River (Station 08GD004)), https://wateroffice.ec.gc.ca/report/data_availability_e.html?type=historical&station=08GD004&parameter_type=Flow+and+Level; Southgate River (Station 08GD010), https://wateroffice.ec.gc.ca/report/data_availability_e.html?type=historical&station=08GD010&parameter_type=Flow+and+Level. Acolite image conversion (Vanhellemont, 2025) is an open access code and can be downloaded from the following link: https://github.com/acolite/acolite/releases/tag/20250114.0.

Acknowledgments

This study took place in the unceded traditional territory of the Homalco First Nation, where Chief Darren Blaney, former Landslide Coordinator Erik Blaney, and Councillor Alison Trenholm led an organized response to the Elliot Creek landslide and helped guide the land-to-sea turbidity monitoring program. We thank David Hutchinson, Curtis Weber, and the Water Survey of Canada staff for rapidly establishing a new gauging station on the Southgate following the Elliot Lake outburst flood. We also thank Suzanne Tank for efforts with in situ data collection in Bute Inlet and Ivan Haigh for assistance in securing funding through the UK-Canada Globalink doctoral exchange program. Finally, we would like to extend thanks to editor Amy East, associate editor Dongfeng Li, Loic Piret and one anonymous reviewer whose comments greatly improved the manuscript in the peer-review process. LPB was supported by the Natural Environmental Council as part of the SPITFIRE doctoral training program (NERC Grant NE/L002531/1) and the UK-Canada Globalink doctoral exchange program (funded by Mitacs and NERC Grant NE/V021095/1). DHS acknowledges funding from the Natural Sciences and Engineering Research Council (NSERC) of Canada (2020-0407), Alberta Innovates. Members of the Hakai Institute acknowledge the Tula Foundation. MJBC acknowledges funding from the Royal Society (DHF\R\231008).

References

Ahmed, R., Wani, G. F., Ahmad, S. T., Sahana, M., Singh, H., & Ahmed, P. (2021). A review of glacial lake expansion and associated glacial lake outburst floods in the Himalayan region. *Earth Systems and Environment*, *5*(3), 695–708. https://doi.org/10.1007/s41748-021-00230-9

Arimitsu, M. L., Piatt, J. F., & Mueter, F. (2016). Influence of glacier runoff on ecosystem structure in Gulf of Alaska Fjords. *Marine Ecology Progress Series*, *560*, 19–40. https://doi.org/10.3354/meps11888

Bailey, L. P., Clare, M. A., Pope, E. L., Haigh, I. D., Cartigny, M. J. B., Talling, P. J., et al. (2023). Predicting turbidity current activity offshore from meltwater-fed river deltas. *Earth and Planetary Science Letters*, *604*, 117977. https://doi.org/10.1016/j.epsl.2022.117977

Bailey, L. P., Clare, M. A., Rosenberger, K. J., Cartigny, M. J. B., Talling, P. J., Paull, C. K., et al. (2021). Preconditioning by sediment accumulation can produce powerful turbidity currents without major external triggers. *Earth and Planetary Science Letters*, *562*, 116845. https://doi.org/10.1016/j.epsl.2021.116845

Bailey, L. P., Shugar, D. H., Tilston, M., Hubbard, S. M., Giesbrecht, I., Del Bel Belluz, J., et al. (2025). Replication data for: Land-to-Sea sediment fluxes from a major Glacial Lake Outburst flood were stepped rather than instantaneous [Dataset]. *Borealis*. https://doi.org/10.5683/SP3/WNRZUD

Bellwald, B., Planke, S., Becker, L. W. M., & Myklebust, R. (2020). Meltwater sediment transport as the dominating process in mid-latitude trough mouth fan formation. *Nature Communications*, *11*(1), 4645. https://doi.org/10.1038/s41467-020-18337-4

Bianchi, T. S., Arndt, S., Austin, W. E. N., Benn, D. I., Bertrand, S., Cui, X., et al. (2020). Fjords as Aquatic Critical Zones (ACZs). *Earth-Science Reviews*, *203*, 103145. https://doi.org/10.1016/j.earscirev.2020.103145

Bornhold, B. D., Ren, P., & Prior, D. B. (1994). High-frequency turbidity currents in British Columbia fjords. *Geo-Marine Letters*, *14*(4), 238–243. https://doi.org/10.1007/BF01274059

Carrivick, J. L., & Tweed, F. S. (2016). A global assessment of the societal impacts of Glacier outburst floods. *Global and Planetary Change*, *144*, 1–16. https://doi.org/10.1016/j.gloplacha.2016.07.001

Clague, J. J., & Evans, S. G. (2000). A review of catastrophic drainage of moraine-dammed lakes in British Columbia. *Quaternary Science Reviews*, *19*(17), 1763–1783. https://doi.org/10.1016/S0277-3791(00)00090-1

Clare, M. A., Hughes Clarke, J. E., Talling, P. J., Cartigny, M. J. B., & Pratomo, D. G. (2016). Preconditioning and triggering of offshore slope failures and turbidity currents revealed by most detailed monitoring yet at a Fjord-head delta. *Earth and Planetary Science Letters*, *450*, 208–220. https://doi.org/10.1016/j.epsl.2016.06.021

Clare, M. A., Le Bas, T., Price, D. M., Hunt, J. E., Sear, D., Cartigny, M. J. B., et al. (2018). Complex and cascading triggering of submarine landslides and turbidity currents at Volcanic Islands revealed from integration of high-resolution onshore and offshore surveys. *Frontiers in Earth Science*, *6*. https://doi.org/10.3389/feart.2018.00223

Conway, K. W., Barrie, J. V., Picard, K., & Bornhold, B. D. (2012). Submarine channel evolution: Active channels in Fjords, British Columbia, Canada. *Geo-Marine Letters*, *32*(4), 301–312. https://doi.org/10.1007/s00367-012-0280-4

Cook, K. L., Andermann, C., Gimbert, F., Adhikari, B. R., & Hovius, N. (2018). Glacial lake outburst floods as drivers of fluvial erosion in the Himalaya. *Science*, *362*(6410), 53–57. https://doi.org/10.1126/science.aat4981

D′Azeredo Orlando, M. T., Galvão, E. S., Sant′Ana Cavichini, A., Gabrig Turbay Rangel, C. V., Pinheiro Orlando, C. G., Grilo, C. F., et al. (2020). Tracing iron ore tailings in the marine environment: An investigation of the Fundão Dam failure. *Chemosphere*, *257*, 127184. https://doi.org/10.1016/j.chemosphere.2020.127184

Deline, P., Gruber, S., Amann, F., Bodin, X., Delaloye, R., Failletaz, J., et al. (2021). Ice loss from glaciers and permafrost and related slope instability in high-mountain regions. In *Snow and ice-related hazards, risks, and disasters* (pp. 501–540). Elsevier. https://doi.org/10.1016/B978-0-12-817129-5.00015-9

Déry, S. J., Stadnyk, T. A., MacDonald, M. K., & Gauli-Sharma, B. (2016). Recent trends and variability in river discharge across Northern Canada. *Hydrology and Earth System Sciences*, *20*(12), 4801–4818. https://doi.org/10.5194/hess-20-4801-2016

Déry, S. J., Stieglitz, M., McKenna, E. C., & Wood, E. F. (2005). Characteristics and trends of river discharge into Hudson, James, and Ungava Bays, 1964–2000. *Journal of Climate*, *18*(14), 2540–2557. https://doi.org/10.1175/JCLI3440.1

do Carmo, F. F., Kamino, L. H. Y., Junior, R. T., de Campos, I. C., do Carmo, F. F., Silvino, G., et al. (2017). Fundão Tailings Dam failures: The environment tragedy of the largest technological disaster of Brazilian mining in global context. *Perspectives in Ecology and Conservation*, *15*(3), 145–151. https://doi.org/10.1016/j.pecon.2017.06.002

Donati, D., Stead, D., Geertsema, M., Bendle, J., Menounos, B., & Borgatti, L. (2022). Kinematic analysis of the 2020 Elliot Creek Landslide, British Columbia, using remote sensing data. *Frontiers in Earth Science*, *10*, 916069. https://doi.org/10.3389/feart.2022.916069

Geertsema, M., Menounos, B., Bullard, G., Carrivick, J. L., Clague, J. J., Dai, C., et al. (2022). The 28 November 2020 landslide, Tsunami, and outburst flood – A hazard cascade associated with rapid deglaciation at Elliot Creek, British Columbia, Canada. *Geophysical Research Letters*, *49*(6), e2021GL096716. https://doi.org/10.1029/2021GL096716

Giesbrecht, I., Tank, S. E., Frazer, G. W., Hood, E., Gonzalez Arriola, S. G., Butman, D. E., et al. (2022). Watershed classification predicts streamflow regime and organic carbon dynamics in the Northeast Pacific Coastal Temperate Rainforest. *Global Biogeochemical Cycles*, *36*(2), e2021GB007047. https://doi.org/10.1029/2021GB007047

Haeussler, P. J., Gulick, S. P. S., McCall, N., Walton, M., Reece, R., Larsen, C., et al. (2018). Submarine deposition of a subaerial landslide in Taan Fiord, Alaska. *Journal of Geophysical Research: Earth Surface*, *123*(10), 2443–2463. https://doi.org/10.1029/2018JF004608

Hage, S., Cartigny, M. J. B., Sumner, E. J., Clare, M. A., Hughes Clarke, J. E., Talling, P. J., et al. (2019). Direct monitoring reveals initiation of turbidity currents from extremely dilute river plumes. *Geophysical Research Letters*, *46*(20), 11310–11320. https://doi.org/10.1029/2019GL084526

Hage, S., Galy, V. V., Cartigny, M. J. B., Heerema, C., Heijnen, M. S., Acikalin, S., et al. (2022). Turbidity currents can dictate organic carbon fluxes across river-fed Fjords: An example from Bute Inlet (BC, Canada). *Journal of Geophysical Research: Biogeosciences*, *127*(6), e2022JG006824. https://doi.org/10.1029/2022JG006824

Harrison, S., Kargel, J. S., Huggel, C., Reynolds, J., Shugar, D. H., Betts, R. A., et al. (2018). Climate change and the global pattern of moraine-dammed Glacial Lake outburst floods. *The Cryosphere*, *12*(4), 1195–1209. https://doi.org/10.5194/tc-12-1195-2018

Heijnen, M. S., Clare, M. A., Cartigny, M. J. B., Talling, P. J., Hage, S., Lintern, D. G., et al. (2020). Rapidly-migrating and internally-generated knickpoints can control submarine channel evolution. *Nature Communications*, *11*(1), 3129. https://doi.org/10.1038/s41467-020-16861-x

Heijnen, M. S., Clare, M. A., Cartigny, M. J. B., Talling, P. J., Hage, S., Pope, E. L., et al. (2022). Fill, flush or shuffle: How is sediment carried through submarine channels to build lobes? *Earth and Planetary Science Letters*, *584*, 117481. https://doi.org/10.1016/j.epsl.2022.117481

Hickin, E. J. (1989). Contemporary Squamish river sediment flux to Howe Sound, British Columbia. *Canadian Journal of Earth Sciences*, *26*(10), 1953–1963. https://doi.org/10.1139/e89-165

Hizzett, J. L., Hughes Clarke, J. E., Sumner, E. J., Cartigny, M. J. B., Talling, P. J., & Clare, M. A. (2018). Which triggers produce the most erosive, frequent, and longest runout turbidity currents on deltas? *Geophysical Research Letters*, *45*(2), 855–863. https://doi.org/10.1002/2017GL075751

Howe, J. A., Austin, W. E. N., Forwick, M., Paetzel, M., Harland, R., & Cage, A. G. (2010). Fjord systems and archives: A review. *Geological Society, London, Special Publications*, *344*(1), 5–15. https://doi.org/10.1144/SP344.2

Hoyal, D. C. J. D., Bursik, M. I., & Atkinson, J. F. (1999). The influence of diffusive convection on sedimentation from buoyant plumes. *Marine Geology*, *159*(1), 205–220. https://doi.org/10.1016/S0025-3227(99)00005-5

Hugonnet, R., McNabb, R., Berthier, E., Menounos, B., Nuth, C., Girod, L., et al. (2021). Accelerated global Glacier mass loss in the early Twenty-First century. *Nature*, *592*(7856), 726–731. https://doi.org/10.1038/s41586-021-03436-z

Islam, K., & Murakami, S. (2021). Global-scale impact analysis of mine Tailings Dam failures: 1915–2020. *Global Environmental Change*, *70*, 102361. https://doi.org/10.1016/j.gloenvcha.2021.102361

Jackson, J. M., Bianucci, L., Hannah, C. G., Carmack, E. C., & Barrette, J. (2021). Deep waters in British Columbia mainland Fjords show rapid warming and deoxygenation from 1951 to 2020. *Geophysical Research Letters*, *48*(3), e2020GL091094. https://doi.org/10.1029/2020GL091094

Jacquet, J., McCoy, S. W., McGrath, D., Nimick, D. A., Fahey, M., O'kuinghttons, J., et al. (2017). Hydrologic and geomorphic changes resulting from episodic Glacial Lake outburst floods: Rio Colonia, Patagonia, Chile. *Geophysical Research Letters*, *44*(2), 854–864. https://doi.org/10.1002/2016GL071374

Koppes, M., & Hallet, B. (2006). Erosion rates during rapid deglaciation in Icy Bay, Alaska. *Journal of Geophysical Research*, *111*(F2). https://doi.org/10.1029/2005JF000349

Koppes, M., Hallet, B., Rignot, E., Mouginot, J., Wellner, J. S., & Boldt, K. (2015). Observed latitudinal variations in erosion as a function of Glacier dynamics. *Nature*, *526*(7571), 100–103. https://doi.org/10.1038/nature15385

Kütter, V. T., Martins, G. S., Brandini, N., Cordeiro, R. C., Almeida, J. P. A., & Marques, E. D. (2023). Impacts of a Tailings dam failure on water quality in the Doce river: The largest environmental disaster in Brazil. *Journal of Trace Elements and Minerals*, *5*, 100084. https://doi.org/10.1016/j.jtemin.2023.100084

Magirl, C. S., Hilldale, R. C., Curran, C. A., Duda, J. J., Straub, T. D., Domanski, M., & Foreman, J. R. (2015). Large-scale dam removal on the Elwha River, Washington, USA: Fluvial sediment load. *Geomorphology*, *246*, 669–686. https://doi.org/10.1016/j.geomorph.2014.12.032

Major, J. J., Bertin, D., Pierson, T. C., Amigo, Á., Iroumé, A., Ulloa, H., & Castro, J. (2016). Extraordinary sediment delivery and rapid geomorphic response following the 2008–2009 eruption of Chaitén Volcano, Chile. *Water Resources Research*, *52*(7), 5075–5094. https://doi.org/10.1002/2015WR018250

Marín, V. H., Tironi, A., Paredes, M. A., & Contreras, M. (2013). Modeling suspended solids in a Northern Chilean Patagonia Glacier-fed fjord: GLOF scenarios under climate change conditions. *Ecological Modelling*, *264*, 7–16. https://doi.org/10.1016/j.ecolmodel.2012.06.017

Marta-Almeida, M., Mendes, R., Amorim, F. N., Cirano, M., & Dias, J. M. (2016). Fundão Dam collapse: Oceanic dispersion of River Doce after the greatest Brazilian environmental accident. *Marine Pollution Bulletin*, *112*(1), 359–364. https://doi.org/10.1016/j.marpolbul.2016.07.039

Meerhoff, E., Castro, L. R., Tapia, F. J., & Pérez-Santos, I. (2019). Hydrographic and biological impacts of a Glacial Lake Outburst flood (GLOF) in a Patagonian fjord. *Estuaries and Coasts*, *42*(1), 132–143. https://doi.org/10.1007/s12237-018-0449-9

Mulder, T., & Syvitski, J. P. M. (1995). Turbidity currents generated at river mouths during exceptional discharges to the world oceans. *The Journal of Geology*, *103*(3), 285–299. https://doi.org/10.1086/629747

Nechad, B., Ruddick, K. G., & Neukermans, G. (2009). Calibration and validation of a generic multisensor algorithm for mapping of turbidity in coastal waters. In *Remote sensing of the ocean, sea ice, and large water regions 2009* (Vol. 7473, pp. 161–171). SPIE. https://doi.org/10.1117/12.830700

Normandeau, A., Dietrich, P., Hughes Clarke, J., Van Wychen, W., Lajeunesse, P., Burgess, D., & Ghienne, J.-F. (2019). Retreat pattern of glaciers controls the occurrence of turbidity currents on high-latitude fjord deltas (Eastern Baffin Island). *Journal of Geophysical Research: Earth Surface*, *124*(6), 1559–1571. https://doi.org/10.1029/2018JF004970

Old, G. H., Lawler, D. M., & Snorrason, Á. (2005). Discharge and suspended sediment dynamics during two Jökulhlaups in the Skaftá river, Iceland. *Earth Surface Processes and Landforms*, *30*(11), 1441–1460. https://doi.org/10.1002/esp.1216

Parsons, J. D., Bush, J. W. M., & Syvitski, J. P. M. (2001). Hyperpycnal plume formation from riverine outflows with small sediment concentrations. *Sedimentology*, *48*(2), 465–478. https://doi.org/10.1046/j.1365-3091.2001.00384.x

Philip, S. Y., Kew, S. F., van Oldenborgh, G. J., Anslow, F. S., Seneviratne, S. I., Vautard, R., et al. (2022). Rapid attribution analysis of the extraordinary heat wave on the Pacific coast of the US and Canada in June 2021. *Earth System Dynamics*, *13*(4), 1689–1713. https://doi.org/10.5194/esd-13-1689-2022

Pickard, G. L., & Giovando, L. F. (1960). Some observations of turbidity in British Columbia inlets. *Limnology & Oceanography*, *5*(2), 162–170. https://doi.org/10.4319/lo.1960.5.2.0162

Pierson, T. C., Major, J. J., Amigo, Á., & Moreno, H. (2013). Acute sedimentation response to rainfall following the explosive phase of the 2008–2009 eruption of Chaitén Volcano, Chile. *Bulletin of Volcanology*, *75*(5), 723. https://doi.org/10.1007/s00445-013-0723-4

Piret, L., Bertrand, S., Moffat, C., Feldens, P., Papenmeier, S., & Arz, H. (2024). Recent ice-contact delta formation in front of Pio XI glacier controls sedimentary processes in Eyre Fjord, Patagonia. *Earth Surface Processes and Landforms*, *49*, 1–15. https://doi.org/10.1002/esp.6012

Piret, L., Bertrand, S., Nguyen, N., Hawkings, J., Rodrigo, C., & Wadham, J. (2022). Long-lasting impacts of a 20th century glacial lake outburst flood on a Patagonian Fjord-river system (Pascua River). *Geomorphology*, *399*, 108080. https://doi.org/10.1016/j.geomorph.2021.108080

Pope, E. L., Cartigny, M. J. B., Clare, M. A., Talling, P. J., Lintern, D. G., Vellinga, A., et al. (2022). First source-to-sink monitoring shows dense head controls sediment flux and runout in turbidity currents. *Science Advances*, *8*(20), eabj3220. https://doi.org/10.1126/sciadv.abj3220

Prior, D. B., Bornhold, B. D., Wiseman, W. J., & Lowe, D. R. (1987). Turbidity current activity in a British Columbia fjord. *Science*, *237*(4820), 1330–1333. https://doi.org/10.1126/science.237.4820.1330

Riihimaki, C. A., MacGregor, K. R., Anderson, R. S., Anderson, S. P., & Loso, M. G. (2005). Sediment evacuation and glacial erosion rates at a small alpine Glacier. *Journal of Geophysical Research*, *110*(F3). https://doi.org/10.1029/2004JF000189

Ritchie, A. C., Warrick, J. A., East, A. E., Magirl, C. S., Stevens, A. W., Bountry, J. A., et al. (2018). Morphodynamic evolution following sediment release from the world's largest dam removal. *Scientific Reports*, *8*(1), 13279. https://doi.org/10.1038/s41598-018-30817-8

Russell, A. J., Roberts, M. J., Fay, H., Marren, P. M., Cassidy, N. J., Tweed, F. S., & Harris, T. (2006). Icelandic Jökulhlaup impacts: Implications for ice-sheet hydrology, sediment transfer and geomorphology. *Geomorphology*, *75*(1), 33–64. https://doi.org/10.1016/j.geomorph.2005.05.018

Sattar, A., Cook, K. L., Rai, S. K., Berthier, E., Allen, S., Rinzin, S., et al. (2025). The Sikkim flood of October 2023: Drivers, causes and impacts of a multihazard cascade. *Science*, *0*(0), eads2659. https://doi.org/10.1126/science.ads2659

Shugar, D. H., Burr, A., Haritashya, U. K., Kargel, J. S., Watson, C. S., Kennedy, M. C., et al. (2020). Rapid worldwide growth of Glacial lakes since 1990. *Nature Climate Change*, *10*(10), 939–945. https://doi.org/10.1038/s41558-020-0855-4

Staines, K. E. H., & Carrivick, J. L. (2015). Geomorphological impact and morphodynamic effects on flow conveyance of the 1999 Jökulhlaup at Sólheimajökull, Iceland. *Earth Surface Processes and Landforms*, *40*(10), 1401–1416. https://doi.org/10.1002/esp.3750

Suchy, K. D., Young, K., Galbraith, M., Perry, R. I., & Costa, M. (2022). Match/mismatch between phytoplankton and Crustacean zooplankton phenology in the Strait of Georgia, Canada. *Frontiers in Marine Science*, *9*. https://doi.org/10.3389/fmars.2022.832684

Taylor, C., Robinson, T. R., Dunning, S., Rachel Carr, J., & Westoby, M. (2023). Glacial lake outburst floods threaten millions globally. *Nature Communications*, *14*(1), 487. https://doi.org/10.1038/s41467-023-36033-x

Tomczyk, A. M., Ewertowski, M. W., & Carrivick, J. L. (2020). Geomorphological impacts of a Glacier lake outburst flood in the high arctic Zackenberg River, NE Greenland. *Journal of Hydrology*, *591*, 125300. https://doi.org/10.1016/j.jhydrol.2020.125300

Tweed, F. S., & Russell, A. J. (1999). Controls on the formation and sudden drainage of glacier-impounded lakes: Implications for Jökulhlaup characteristics. *Progress in Physical Geography: Earth and Environment*, *23*(1), 79–110. https://doi.org/10.1177/030913339902300104

Vandekerkhove, E., Bertrand, S., Crescenzi Lanna, E., Reid, B., & Pantoja, S. (2020). Modern sedimentary processes at the heads of Martínez channel and Steffen Fjord, Chilean Patagonia. *Marine Geology*, *419*, 106076. https://doi.org/10.1016/j.margeo.2019.106076

Vandekerkhove, E., Bertrand, S., Torrejón, F., Kylander, M. E., Reid, B., & Saunders, K. M. (2021). Signature of modern glacial lake outburst floods in fjord sediments (Baker River, Southern Chile). *Sedimentology*, *68*(6), 2798–2819. https://doi.org/10.1111/sed.12874

Vanhellemont, Q. (2019a). Adaptation of the dark spectrum fitting atmospheric correction for aquatic applications of the Landsat and Sentinel-2 archives. *Remote Sensing of Environment*, *225*, 175–192. https://doi.org/10.1016/j.rse.2019.03.010

Vanhellemont, Q. (2019b). Daily metre-scale mapping of water turbidity using CubeSat imagery. *Optics Express*, *27*(20), A1372–A1399. https://doi.org/10.1364/OE.27.0A1372

Vanhellemont, Q. (2020). Sensitivity analysis of the dark spectrum fitting atmospheric correction for metre- and decametre-scale satellite imagery using autonomous hyperspectral radiometry. *Optics Express*, *28*(20), 29948. https://doi.org/10.1364/OE.397456

Vanhellemont, Q. (2025). Acolite. Python [Software]. https://github.com/acolite/acolite

Vanhellemont, Q., & Ruddick, K. (2014). Turbid wakes associated with offshore wind turbines observed with Landsat 8. *Remote Sensing of Environment*, *145*, 105–115. https://doi.org/10.1016/j.rse.2014.01.009

Vanhellemont, Q., & Ruddick, K. (2018). Atmospheric correction of metre-scale optical satellite data for inland and coastal water applications. *Remote Sensing of Environment*, *216*, 586–597. https://doi.org/10.1016/j.rse.2018.07.015

Veh, G., Korup, O., & Walz, A. (2020). Hazard from Himalayan glacier lake outburst floods. *Proceedings of the National Academy of Sciences*, *117*(2), 907–912. https://doi.org/10.1073/pnas.1914898117

Warrick, J. A., Bountry, J. A., East, A. E., Magirl, C. S., Randle, T. J., Gelfenbaum, G., et al. (2015). Large-scale dam removal on the Elwha River, Washington, USA: Source-to-sink sediment budget and synthesis. *Geomorphology*, *246*, 729–750. https://doi.org/10.1016/j.geomorph.2015.01.010

Wilson, R., Glasser, N. F., Reynolds, J. M., Harrison, S., Anacona, P. I., Schaefer, M., & Shannon, S. (2018). Glacial lakes of the central and Patagonian Andes. *Global and Planetary Change*, *162*, 275–291. https://doi.org/10.1016/j.gloplacha.2018.01.004

Wright, L. D. (1977). Sediment transport and deposition at river mouths: A synthesis. *GSA Bulletin*, *88*(6), 857–868. https://doi.org/10.1130/0016-7606

Xu, M., Bogen, J., Wang, Z., Bønsnes, T. E., & Gytri, S. (2015). Pro-Glacial Lake Sedimentation From Jökulhlaups (GLOF), Blåmannsisen, Northern Norway. *Earth Surface Processes and Landforms*, *40*(5), 654–665. https://doi.org/10.1002/esp.3664

Zhang, T., Li, D., East, A. E., Walling, D. E., Lane, S., Overeem, I., et al. (2022). Warming-driven erosion and sediment transport in cold regions. *Nature Reviews Earth & Environment*, *3*(12), 832–851. https://doi.org/10.1038/s43017-022-00362-0